ADVANCED MATERIALS INTERFACES
Open Access
www.advmatinterfaces.de



# Stability of Immobilized Chemosensor-Filled Vesicles on Anti-Fouling Polymer Brush Surfaces

*Wenwu Yang, Jiangxiong Xiao, Bingquan Yang, George Mathew, Andreas H. Schäfer, and Michael Hirtz**

**The characterization of phospholipid membrane permeability for small molecules is crucial for many applications in drug discovery and biomedical research in general. Here, chemosensor-laden vesicles offer an attractive platform for permeability assays. In this work, the stability of immobilized chemosensor-filled vesicles is explored on anti-fouling polymer brush surfaces for potential use in monitoring small molecule membrane permeability. The study focuses on the development of a method for immobilizing sensor-loaded vesicles into arbitrary patterns on surfaces and characterizing their stability under changing temperatures and compositions. As substrate to enable intact, long-term stable vesicle immobilization reactive polymer brushes with anti-fouling properties are used. Utilizing microchannel cantilever spotting, biotin moieties are introduced on the polymer brush surface, enabling stable tethering of vesicles through streptavidin-biotin interactions. The immobilized vesicles are monitored through fluorescence microscopy for their response to analytes under changing environmental parameters and vesicle composition. A higher stability of immobilized vesicles compared to free-floating ones is observed, with permeability only at elevated temperatures. By tuning vesicle compositions, permeability at lower temperatures can be raised again. Overall, the study provides insights into a novel approach for vesicle immobilization, showcasing the potential of surface-bound vesicles for applications in microfluidic systems and as biosensors in various assays.**

## 1. Introduction

The permeability of cell membranes for various substances is of uttermost importance for vital functions of cells, such as the exchange of nutrients, metabolites, and signaling molecules, as well as for influencing cells by pharmaceutical drugs.[1,2] Especially for the latter, biomimetic phospholipid membrane models are frequently used for screening the transfer properties of potential drugs. Here, in particular, two methods are frequently used, the parallel artificial membrane permeability assay (PAMPA), and the Caco-2 cell assay.[3] PAMPA uses artificial or tissue-extracted lipid membranes separating two compartments to assess permeability. In contrast, in the Caco-2 cell assay, a confluent monolayer of cells is used to mimic a biological barrier between two compartments. Both techniques have different strengths and challenges, depending on the specific application.[4] However, in particular for high-throughput applications, PAMPA seems prevalent as of the more complex setup when living cells are involved in an assay.[5]

Recently, an interesting approach using artificial indicators encapsulated in vesicles was demonstrated.[6] In this fluorescent artificial receptor-based membrane assay (FARMA), vesicles are loaded with a sensor consisting of a cucurbituril hosting a dye molecule. If the sensor is reached by an analyte molecule passing the vesicle membrane from the outside, it can be inserted into the sensor and quench fluorescence. In FARMA, the assessment of permeability does not rely on two separate compartments, but rather utilizes the vesicles as many self-contained sensing compartments.

Immobilization of chemical sensors to substrates can bring many benefits in applications. First, it makes the sensor resistant to washing, that is, enables the exchange of sample solution or subsequent incubation steps without losing sensor material. In particular, it becomes possible to use immobilized chemical sensor arrays in microfluidic chips, e.g. for real-time monitoring of streaming sample media. Furthermore, it can ease handling in comparison to a bulk solution, as the chemical sensor is attached to a solid substrate. It has also been shown, that indicator displacement assays (IDA) can gain sensitivity by immobilization, as the possibility to wash allows for the removal of fluorescent interfering with the readout and the comparably low number of molecules in an immo-

W. Yang, J. Xiao, B. Yang, G. Mathew, M. Hirtz
Institute of Nanotechnology (INT) & Karlsruhe Nano Micro Facility (KNMFi)
Kaiserstraße 12, 76131 Karlsruhe, Germany
E-mail: michael.hirtz@kit.edu
A. H. Schäfer
nanoAnalytics GmbH
Heisenbergstraße 11, 48149 Münster, Germany

The ORCID identification number(s) for the author(s) of this article can be found under https://doi.org/10.1002/admi.202400200



**DOI: 10.1002/admi.202400200**

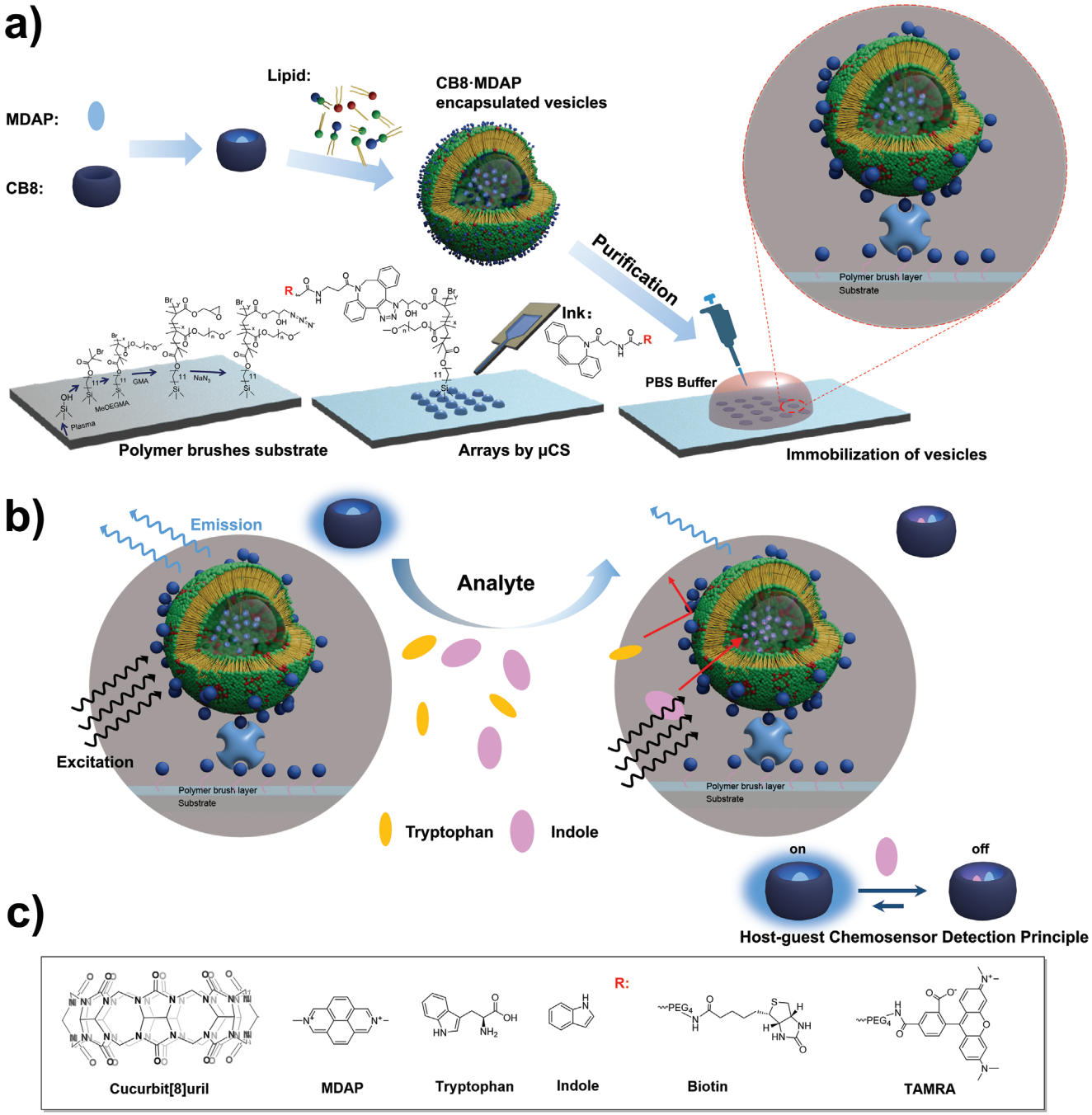


**Figure 1.** a) Scheme of the preparation of the vesicle-encapsulated chemosensor, synthesis of the polymer brush, spotting of a biotin array, and immobilization of the chemosensor vesicles. b) Principle of analyte detection. Indole permeates lipid membranes much more efficiently than tryptophane and is able to reach the encapsulated chemosensor, turning off the fluorescence signal. c) Structure of the chemicals used in the chemosensor, analytes, and inks for spotting. Figure partly created with BioRender.com.

bilized monolayer (compared to a bulk solution) can detect already efficiently at low analyte concentration (allowing also for low volume applications).[7] In general, the immobilized artificial vesicles can also be exploited as nanoreactors or for cascade reactions.[8–11]

In this work, we introduce an approach for the immobilization of sensor-loaded vesicles into arbitrary patterns on surfaces and characterize their stability under changes in temperature and composition. The overall approach is depicted in **Figure 1**.

The general approach for generating surface-bound vesicles is by tethering them to a substrate by a suitable linker. As vesicles tend to spread into supported lipid bilayers (SLB) on contact with solid surfaces, a passivation of the surface is needed to keep vesicles intact. This can be achieved with different

self-assembled monolayers (SAMs),[12] by bovine serum albumin (BSA),[13] or even by a preformed SLB (though here eventually vesicles still can merge into the supporting layer).[14] At the same time, specific binding sides are needed, to allow a stable tethering to the substrate. Here polymer brushes can be an interesting alternative anti-fouling surface, as they offer a broad range of options in regard to chemistry, structure, and hydrophilicity, which all play a role in biofouling.[15] Recently, the Rodriguez-Emmenegger group demonstrated the immobilization of vesicles on N-(2-hydroxypropyl) methacrylamide (HPMA) / N-(3-methacrylamidopropyl)-N,N-dimethyldodecan-1-aminiumiodide (C12+) diblock copolymer brushes via electrostatic attraction and bio-inspired "harpooning" of the hydrophobic C12+ tails into the vesicle membrane.[16] To introduce specific and localized binding sites, we chose reactive polymer brushes as substrates, for the excellent anti-fouling properties, while still comprising click-chemistry moieties allowing for selective modification to introduce tethering sides at the places desired.[17–22] These are introduced in our strategy via microchannel cantilever spotting (μCS), allowing for arbitrary surface patterns of biotin moieties to be introduced to the polymer brush. As chemosensor components cucurbit[8]uril (CB8) and 2,7-dimethyldiazapyrenium (MDAP) were chosen to obtain CB8·MDAP. This chemosensor has remarkable host-guest interaction capabilities, particularly its ability to form stable inclusion complexes with a wide range of guest molecules.[23,24] Generally, it offers a highly tunable and versatile platform for molecular recognition, making it an attractive candidate for constructing chemosensors with enhanced selectivity and sensitivity.[25] The CB8·MDAP detection principle is based on quenching of fluorescence by the analyte. While the MDAP inside the CB8 is fluorescent active ("on" state), there is enough space inside the cavity to accommodate a matching analyte. Once the analyte enters the CB8, it quenches the MDAP fluorescence ("off" state), with the drop in fluorescence being the monitored detection signal (Figure 1b). After preparation of the sensor-laden vesicle, these can be incubated onto the patterned polymer brush sample, allowing for self-assembly of the vesicles over a biotin-streptavidin sandwich. The immobilized vesicle arrays can then be monitored by fluorescence microscopy for their response to analytes or changes in environmental parameters.

## 2. Results and Discussion

### 2.1. Substrate Preparation and Characterization

As substrates for vesicle immobilization, glass surfaces with reactive di-block polymer brushes were prepared, because of their excellent antifouling properties and ability to couple specific binding sites for the vesicle tethering via strain-promoted alkyne-azide cycloaddition (SPAAC).[18] These brushes consist of an antifouling base block of poly(ethylene glycol) methyl ether methacrylate (MeOEGMA) and a top block of glycidyl methacrylate (GMA), with the top block being modified by sodium azide to obtain the final azido-functionalized polymer brush, allowing click-chemistry coupling of dibenzocyclooctin (DBCO) moiety bearing compounds (Figure 1a).

A successful synthesis of the polymer brush was monitored over the different steps by X-ray photoelectron spectroscopy (XPS), atomic force microscopy (AFM), and water contact angle (WCA) measurements. The WCA changes after each synthesis step (**Figure 2a**), from (56.2 ± 0.4)° (bare glass), to (72.6 ± 0.1)° (after initiator is grafted), to (51.0 ± 0.1)° (after MeOEGMA segment is added to the glass surface), to (54.8 ± 0.4)° (after GMA segment is grafted), to a final value of (66.2 ± 0.2)° (after modification with sodium azide). XPS confirms the step-by-step synthesis with corroborating chemical data (Figure 2b,c). The thicknesses of the base- and top block were determined with AFM by introducing a scratch to the brush film. After the base block is synthesized, the film thickness reaches (16.5 ± 1.5) nm. After grafting of the top block, the thickness rises to (38.9 ± 2.3) nm, indicating a thickness of ≈22 nm for the top block (Figure S1, Supporting Information).

Finally, the functionality of the polymer brush was evaluated by spotting a fluorescent dye (DBCO-modified carboxytetramethylrhodamin (DBCO-TAMRA)) and biotin-DBCO (to allow selective protein binding) via μCS (Figure 2d–f). The resulting patterns can be clearly observed in fluorescence microscopy and are resistant to washing, thus showing a covalent attachment to the polymer brush. While the biotin-DBCO patterns are initially non-fluorescent, upon incubation with labeled protein (FITC-streptavidin), they become clearly visible in the green fluorescence channel (Figure 2f). As the streptavidin incubation was performed without any blocking steps, the clear emergence of the pattern also showed the excellent anti-fouling properties of the polymer brushes. Overall, the results confirm the successful preparation and functionality of the di-block polymer brushes.

### 2.2. Lipid Vesicle Preparation and Characterization

The encapsulation of the CU-based chemosensors into lipid vesicles was achieved by freeze-thaw cycling and extrusion (**Figure 3a**). As the lipid profile of vesicles has a significant impact on their phase transition temperature and stability,[26] different phospholipid mixtures of 1,2-dioleoyl-sn-glycero-3-phosphocholine (DOPC) and 1,2-dipalmitoyl-sn-glycero-3-phosphocholine (DPPC) were used in the preparations to assess their prospects for the chemosensor encapsulation and surface tethering. The chemical structures of all used phospholipids and the chemosensor components (Cucurbit[8]uril (CB8) and 2,7-dimethyldiazapyrenium (MDAP)) are shown in Figure 3b.

All prepared vesicles contain ≈10% 1,2-dioleoyl-sn-glycero-3-phosphoethanolamine-N-(cap biotinyl) (Biotin cap PE) to enable their immobilization onto spotted biotin features on the polymer brush via a streptavidin linker. Dynamic light scattering (DLS) measurements revealed a smooth distribution of vesicle size ≈100 nm (Figure 3c). As a test of the functionality of the encapsulation, the vesicles were probed with a non-membrane crossing analyte (tryptophan) and a fast membrane crossing analyte (indole) in bulk solutions (vesicles freely floating in solution) while the optical activity was measured by fluorescence spectroscopy (Figure 3d). Adding indole to the vesicle (DPPC:Biotin cap PE 4:1) solution has negligible influence on the fluorescence activity, showing that the chemosensor is indeed successfully encapsulated into the vesicles and therefore shielded from interaction with the analyte by the membrane barrier. This also indicates

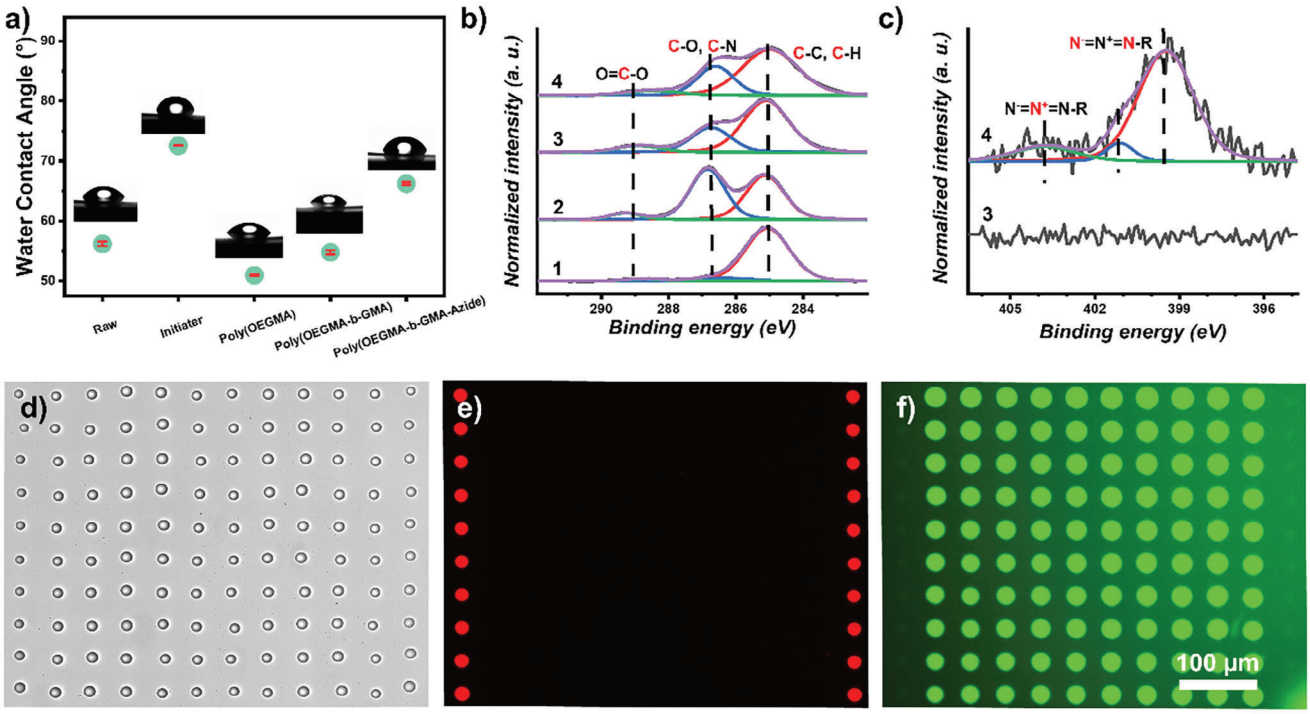


**Figure 2.** Substrate characterization and spotting tests. a) Change in WCA over the different polymer brush synthesis steps. b) XPS characterization at C 1s region of the different stages of polymer brush synthesis. 1) ATRP initiator coated surface, 2) poly(OEGMA) coated surface, 3) poly(OEGMA-b-GMA) surface, 4) poly[OEGMA-b(3-azido-2-hydroxypropyl methacrylate)] coated surface. c) XPS characterization at N 1s region of poly(OEGMA-b-GMA) 3 before and 4 after azide functionalization. The components resulting from corresponding chemical species are highlighted in red. All spectra are normalized to the corresponding maximum intensity. d) A multicomponent microarray with TAMRA- (left- and rightmost columns) and biotin features (middle columns) directly after spotting. After washing the sample, the TAMRA-containing columns are visible in fluorescence microscopy e) red channel) and after incubation with fluorescently labeled streptavidin also the biotin columns f) green channel).

the complete elimination of non-encapsulated chemosensor during vesicle fabrication, as fluorescence of the free chemosensor would be turned off. When indole is added, a sharp decrease of the fluorescence signal is observed indicating that the analyte can rapidly enter into the vesicles and turn off the fluorescence of the chemosensor.

### 2.3. Microarraying and Immobilization of Vesicles

Having established the integrity and functionality of the vesicles in bulk, the vesicle solution is used for a patterned immobilization of sensor-laden vesicles onto surfaces (**Figure 4**).

For this, first, a Biotin-DBCO ink is spotted into a regular 5 × 5 dot array via µCS. After coupling the biotin moieties to the polymer brushes, the sample is rinsed to remove excess ink. On such a prepared biotin array, a streptavidin solution in phosphate-buffered saline (PBS) is incubated onto the sample for 30 min to allow the streptavidin linker to attach to the biotin-binding sites. After this, the sample is washed again and incubated with the desired vesicle solution for ≈20 h. Finally, the samples are washed with PBS to remove the vesicle solution and unbound vesicles. A typical result of such a procedure is shown in Figure 4b–d. The spotted array becomes clearly visible in fluorescence microscopy, indicating the successful site-specific immobilization of the chemosensor-laden vesicles.

### 2.4. Monitoring of Emission in Immobilized Vesicles

With the strategy for vesicle immobilization established, studying stability and sensing capability was conducted. First, immobilized vesicles containing DPPC:Biotin cap PE 4:1 were probed with indole (500 µM) at different temperatures and the fluorescence signal from the arrays was monitored for 60 min (**Figure 5**).

From the experiment, it became evident that the indole is not able to significantly cross the membrane barrier of the vesicles up to≈50 °C, as no significant decrease in fluorescence signal is observed within 60 min (Figure 5b). In the 55 °C case, some decrease in spot-to-background intensity was visible. For a further temperature rise up to 65 °C, a roughly linear decrease in fluorescence intensity was observed (this was then followed up until 170 min, Figure S2, Supporting Information), indicating that the vesicle membrane gets disturbed enough for the indole to permeate through the membrane only at comparably high temperatures. This points to a significantly more stable membrane in the immobilized vesicles compared to the free-floating vesicles, as a bulk solution of the same vesicles decreases in fluorescence even at room temperature (Figure 3d).

Given the high transition temperature of DPPC (41.3 °C),[27] DOPC (with a much lower transition temperature of −16.5 °C)[28] was added as a component to the vesicle in an attempt to raise the permeability of the surface-bound vesicles at lower temperatures.

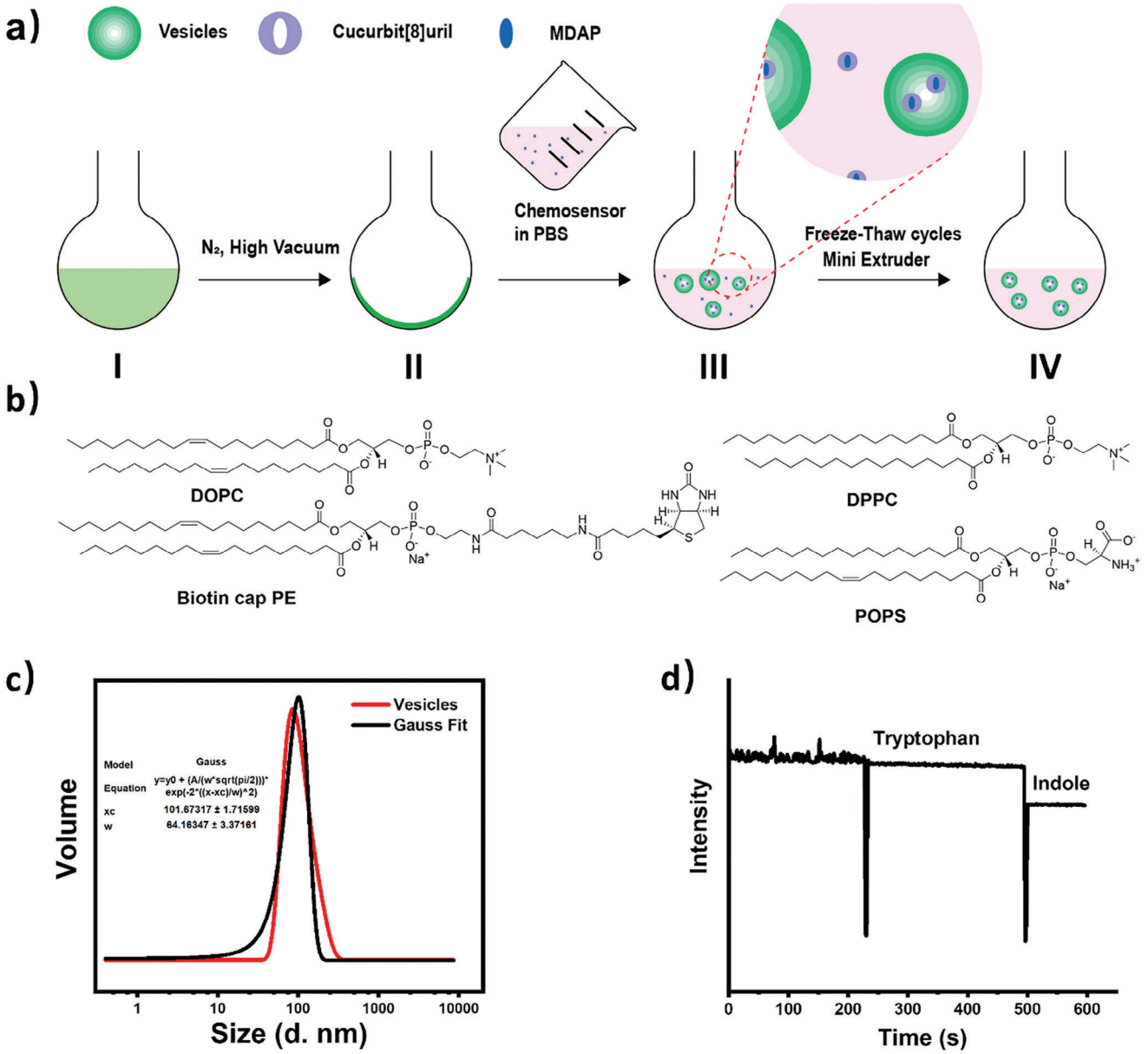


**Figure 3.** Vesicle preparation and characterization. a) Procedure for vesicle production: I) Lipid in chloroform solution, II) "lipid cake" formation by evaporation, III) vesicles are formed by hydration, and IV) vesicles in solution after purification. b) Chemical structure of the phospholipids used in this work. c) DLS determination of vesicle size in the purified solution, showing a narrow distribution. A Gauss model fit results (101.7 ± 32.7) nm for the vesicle size. d) Fluorescence spectroscopy of the purified vesicle solution added with 10 μM, 10 μL tryptophan, followed by 10 mM, 10 μL indole. Only with the addition of indole, does the fluorescence signal show a sharp drop, indicating there are no unencapsulated CB8·MDAP species in the purified vesicle solution.

Here, vesicles with a lipid mixture of DPPC:DOPC:Biotin cap PE 2:2:1 were trialed at room temperature (**Figure 6**).

As intended, the immobilized vesicles with the DOPC addition are now susceptible to indole and show a near-linear decrease in fluorescence intensity under indole incubation even at room temperature. Still, the integrity and stability of the vesicles are preserved, as negative controls (incubation with PBS and with 500 μm tryptophan) show only negligible loss in fluorescence intensity. Passive diffusion or permeation of small non-charged compounds can be regarded as conforming to a modified version of Fick's law and can be described by first-order kinetics.[29] Under the assumption that each analyte molecule entering a vesicle would be taken up by a CB8·MDAP, thus giving a change in the fluorescence signal, and neglecting analyte molecules that might detach again after complexing with CB8·MDAP and that complexed analyte molecules cannot exit the vesicle again, this kinetic process can be effectively modeled by fitting exponential curves to obtain the observed permeation rate ($k_{obs}$). In our setup, we obtain $k_{obs} = 0.0067\ min^{-1}$. Utilizing a previously established permeation model for liposomes,[30] which expresses the

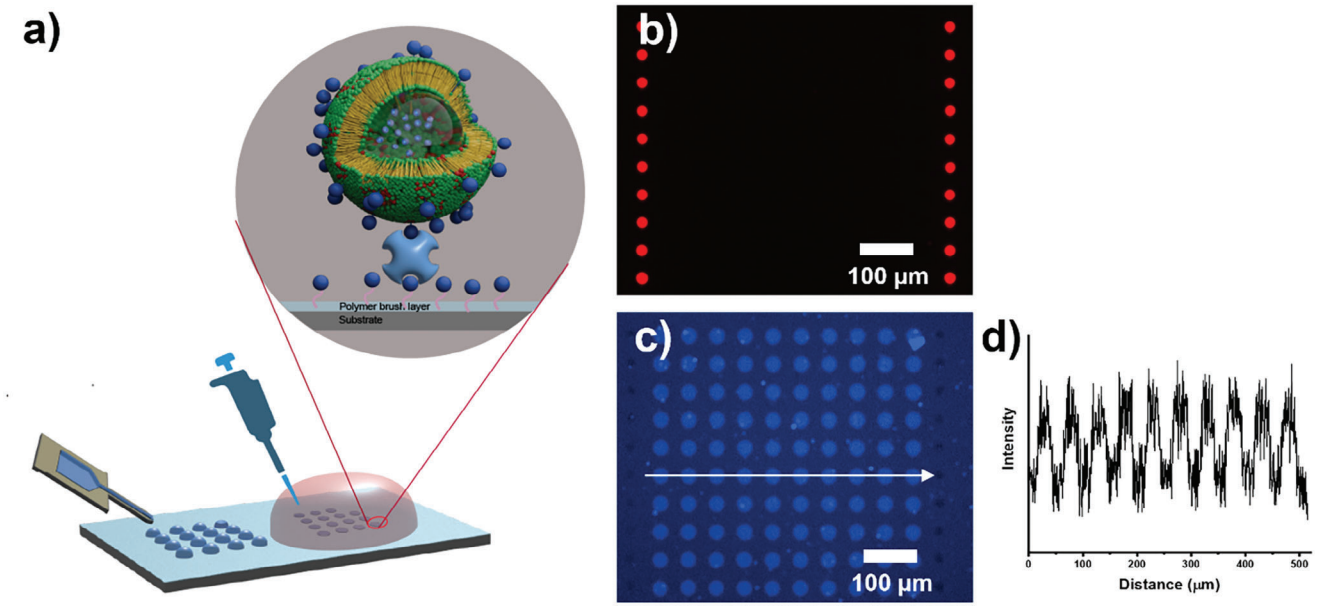


**Figure 4.** Immobilization of vesicles on the polymer brush surface. a) Scheme of the approach and depiction of vesicle binding over biotin-streptavidin linker. b) Fluorescence microscopy image showing the TAMRA marker columns (red channel) and c) the immobilized vesicles (blue channel). d) Intensity profile along the arrow marked in c). Figure partly created with BioRender.com.

apparent permeability coefficients ($P_{app}$) by the permeation rate constant ($k_p$) and vesicle radius ($r$), where $k_p$ can be substituted by $k_{obs}$ and the concentrations of indole ($c_{Indole}$) and CB8·MDAP ($c_{CB8·MDAP}$) respectively we obtain following expression for $P_{app}$:

$$P_{app} = k_p \cdot (r/3) = k_{obs}/c_{Indole} \cdot c_{CB8·MDAP} \cdot (r/3) \quad (1)$$

For the experiment with indole on DPPC:DOPC:Biotin cap PE 2:2:1 vesicles we obtain (with $r$ = 100 nm, $c_{Indole}$ = 500 µM, and $c_{CB8·MDAP}$ = 200 µM) $P_{app}$ = 7.4·10$^{-11}$ cm·s$^{-1}$. This value is in a reasonable range for what would be expected from the vesicle system based on comparison to other lipid vesicles.[30]

## 3. Conclusion

Our experiments demonstrate a successful strategy for the immobilization of intact vesicles with encapsulated chemosensors onto anti-fouling surfaces, with high stability of the vesicles in regard to washing and incubation steps and in arbitrary patterns such as, for example, array formats. The immobilization makes it feasible to use these setups for incorporation into microfluidic systems and enables real-time monitoring in flowing analyte streams. Interestingly, our experiments indicate a higher membrane stability / lower membrane permeability in surface-bound vesicles as evidenced by the need for raising the temperature for sensing indole compared to the bulk solution of vesicles of the same composition. By tuning the vesicle composition by adding low transition temperature phospholipids, the sensing

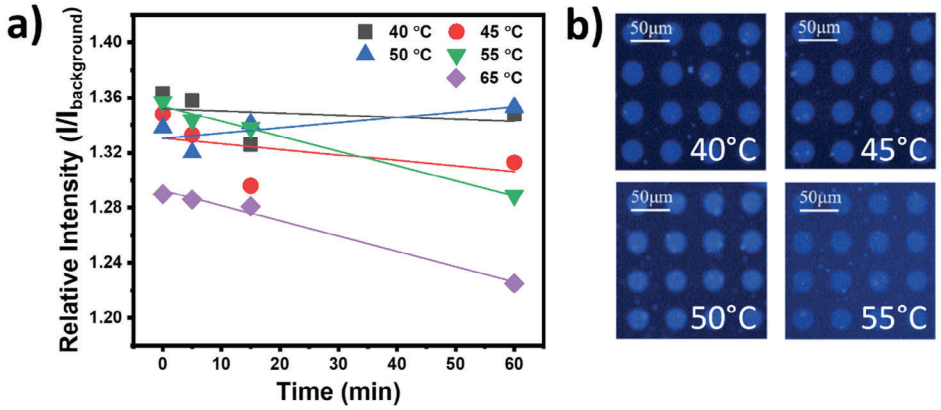


**Figure 5.** Temperature influence on vesicle membrane permeability for indole. a) Relative fluorescence intensity of array spots versus substrate background over time for different temperatures indole incubation on DPPC:Biotin cap PE 4:1 vesicles. b) Endpoint fluorescence images of vesicle arrays incubated at different temperatures.

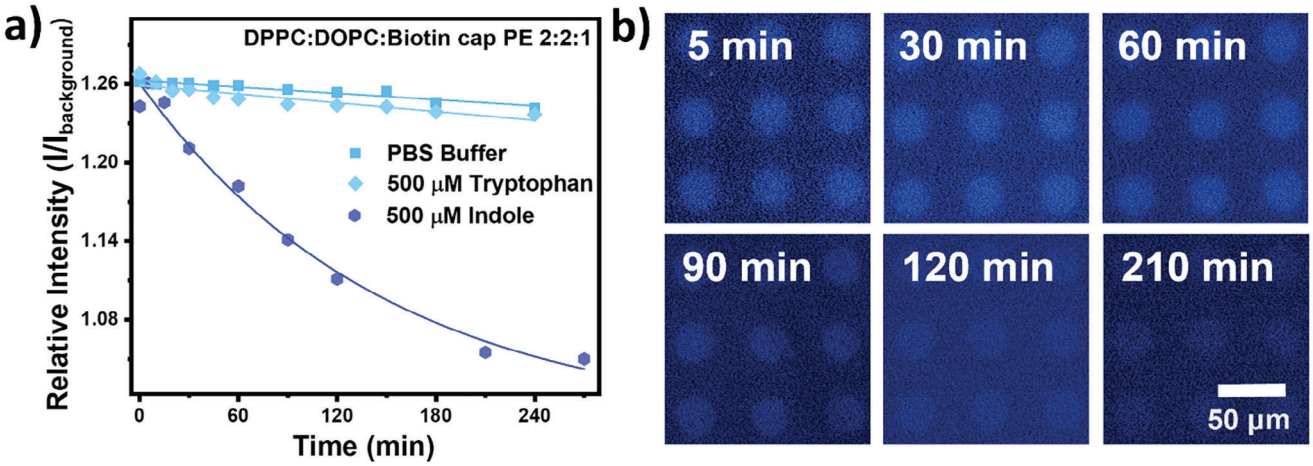


**Figure 6.** Composition influence on vesicle membrane permeability for indole. a) Relative fluorescence intensity of array spots versus substrate background over time for room temperature incubation of indole and as controls incubation of pure PBS, and tryptophan on immobilized DPPC:DOPC:Biotin cap PE 2:2:1 vesicles. b) Fluorescence images of vesicle arrays incubated with indole at room temperature at different time points.

temperature could be brought back to room temperature. Overall, the experiments presented here offer a new route for future applications in assays for membrane permeability and biosensors for membrane-permeable compounds in microfluidic systems.

## 4. Experimental Section

*Materials*: All chemicals in this study were used as received, without any purification procedures. [11-(2-Bromo-2-Methyl) Propionyloxy] Undecyltrichlorosilane (ATRP-initiator) was provided by Cymit (Spain). CuBr, $CuBr_2$, $NaN_3$, 2,2′-bipyridyl, Poly(ethylene glycol) methyl ether methacrylate (Mn = 300 g $mol^{-1}$, MeOEGMA) and glycidyl methacrylate (GMA), N,N-dimethylformamide (DMF), dichloromethane, chloroform, methanol, ethanol, acetone, phosphatebuffered saline (PBS), streptavidin, and toluene were purchased from Sigma-Aldrich (Germany). Dibenzylcyclooctyne-PEG4-5/6-tetramethylrhodamine (DBCO-TAMRA) and dibenzylcyclooctyne-PEG4-biotin conjugate (DBCO-Biotin) were obtained from Jena Bioscience (Germany). Aluminum oxide 90 basic for column chromatography was purchased from Carl Roth (Germany). The phospholipids 1,2-dioleoyl-sn-glycero-3-phosphocholine (DOPC), 1,2-dipalmitoyl-sn-glycero-3-phosphocholine (DPPC), 1,2-dioleoyl-sn-glycero-3-phosphoethanolamine-N-(cap biotinyl) (Biotin cap PE) were used in vesicle fabrication. All lipids were purchased from Avanti Polar Lipids, USA. Deionized water was produced in the lab by an Arium Pro system from Sartorius (Germany).

*Substrate Preparation*: The detailed preparation protocol for the antifouling polymer brush functionalized slides is outlined in the literature.[18] First, the surface is functionalized with a self-assembled monolayer (SAM) comprising an ATRP initiator. The procedure is as follows: glass coverslips were first sonicated in chloroform, ethanol, and deionized water for 5 min, respectively. After being dried under a nitrogen stream, the glass slides were hydroxylated by oxygen plasma (10 sccm $O_2$, 0.2 mbar, 100 W, 20 min, ATTO system, Diener Electronics, Germany). Without delay, the slides were then immersed in a freshly prepared they were immersed in a 1 mg $mL^{-1}$ solution of (11-(2-bromo-2methyl)propionyloxy)undecyltrichlorosilane in anhydrous toluene and kept in a dry environment for 3 h. Subsequently, the slides were rinsed with toluene, ethanol, and deionized water for 5 min respectively, and blown with nitrogen for drying.

The polymer brushes employed in this study exhibit a diblock hierarchical structure, comprising an antifouling bottom layer responsible for the antifouling property, and a top layer modified with azide groups. To prepare the bottom polymer block via surface initiator-ATRP, 7.5 mL of deoxygenated methanol, bubbled with nitrogen for 1 h, was added to a pre-deoxygenated round-bottom flask containing 2,2′-bipyridyl (231.6 mg, 1480.7 µmol), $CuBr_2$ (25.1 mg, 112 µmol), and CuBr (82.3 mg, 573.7 µmol). The catalyst solution was obtained after stirring until the contents fully dissolved. MeOEGMA (8.85 g, 28.5 mmol) (inhibitors were eliminated by passing the monomers through an alumina column) and 7.5 mL of deionized water, deoxygenated with nitrogen for 1 h, were added to the flask containing the catalyst solution and the resulting solution was transferred to a separate nitrogen-filled reactor coated with ATRP initiator on the substrate. After reacting for 20 min at 30 °C, the substrates were removed from the reacting solution to stop the polymerization. Then the substrates were rinsed with ethanol, deionized water, and finally dried under a stream of nitrogen.

Next, the top polymer block was prepared via macroinitiator-ATRP of glycidyl methacrylate (GMA) using poly(OEGMA) brushes as macroinitiators, followed by nucleophilic ring-opening of epoxide with azide. N, N-Dimethylformamide (DMF, 15 mL), 2,2′-bipyridyl (286.4 mg, 1832.4 µmol), $CuBr_2$ (32.6 mg, 146.6 µmol), and GMA (10 mL, 73.1 mmol) were deoxygenated by bubbling with nitrogen for 1 h. Subsequently, CuBr (105.7 mg, 737.3 µmol) was added and the mixture was stirred until fully dissolved, then transferred to the reactor containing substrates coated with poly(OEGMA). After reacting at 60 °C for 6 h, the substrates were removed from the reactor, rinsed twice with DMF and dichloromethane, and dried under a nitrogen stream.

To finally obtain the azido functionalized diblock polymer brushes, a nucleophilic epoxide ring-opening with azide was carried out by immersing the substrates into a solution of $NaN_3$ (3.4 mg $mL^{-1}$) in anhydrous DMF at 60 °C for 24 h. Afterward, the substrates were rinsed with DMF, ethanol, and water twice each and dried with nitrogen.

*Water Contact Angle (WCA) Measurements*: The static water contact angles were performed on an OCA-20 contact angle analyzer (DataPhysics Instruments GmbH, Germany) at room temperature. Briefly, the data recording involved depositing a 3 µL water droplet onto the surface, with each measurement being repeated three times per sample to ascertain the mean standard deviation.

*X-Ray Photoelectron Spectroscopy (XPS)*: XPS measurements were conducted by a Thermo VG Scientific, type K-Alpha in an ultra-high vacuum environment with a base pressure of $1 \times 10^{-9}$ mbar. Core-level spectra were obtained using monochromatic Al-$K_\alpha$ radiation (1486.6 eV), 400 µm spot size. The energy scale of the spectrometer was calibrated using copper, silver, and gold reference samples according to ISO15472:2001.

Initially, survey XP spectra were acquired for each sample, revealing no unexpected contaminations. Subsequently, detailed XP spectra for C 1s and N 1s were recorded. The CasaXPS software was employed for the

precise determination of C 1s and N 1s line positions and necessary corrections. Line correction was calibrated to the C 1s peak at 285.0 eV.

*Spotting of Microarrays*: The DBCO-Biotin ink contained 80 vol % 1 mg·mL$^{-1}$ of DBCO-Biotin in DMSO and 20 vol % glycerol. Reference ink contained 80 vol % 1 mg·mL-1 of DBCO-TAMRA in DMSO and 20 vol. % glycerol. Glycerol was introduced to the ink to mitigate ink evaporation during printing.

The patterning of DBCO-Biotin and DBCO-TAMRA on polymer brushes was performed on an NLP 2000 system (NanoInk, USA) by μCS. A 0.5 μL of the prepared ink was deposited onto the reservoir of the microchannel cantilever (SPT-S-C30S, Bioforce Nanosciences). The cantilever was then affixed to the lithography setup, and spotting occurred by engaging the tip with the prepared polymer brushes coated surface for a defined dwell time (≈1.5–3 s for DBCO-Biotin ink, ≈0.5–2 s for DBCO-TAMRA ink) under controlled humidity conditions of 40–50% RH to control the quality of the patterns. Dot patterns were designed of 10 × 10 spot arrays with a pitch of 50 μm in each direction. After writing, the substrates were allowed to rest for 15 min to promote binding, followed by rinsing with deionized water to get rid of excess ink and then dried by nitrogen blow.

*Preparation of Vesicles*: All the vesicles in this work were fabricated by lipid film rehydrating.[31] A scheme of the process to prepare CB8·MDAP encapsulating liposomes with biotin-binding moieties on the surface is shown in Figure 3a. A 10 mg mL$^{-1}$ DPPC in chloroform solution was mixed with a 10 mg mL$^{-1}$ Biotin cap PE solution at a molar ratio of 4:1. The "lipid cake" was obtained after the mixture was blown by nitrogen for 1 h. Then, the lipid cake was super-dried under a low vacuum overnight. Subsequently, the chemosensor (CB8·MDAP, 220 μM) solution was prepared by dissolving CB8 in a PBS solution containing 220 μM MDAP (a slight excess of MDAP was employed to ensure complete complexation of the CB8) assisted by stirring and oil bath, 45 °C, was introduced into the lipid cake. The resulting mixture was stirred at 400 rpm at 55 °C for 1 h to facilitate the self-assembly of lipids into artificial vesicles, followed by 13 freeze-thaw cycles to enhance encapsulation efficiency, Mini Extruder (Avanti Polar Lipids, USA) to control the size of the vesicles ($r$ = 100 nm) and size-exclusion chromatography (NAP-25 column) to get rid of unencapsulated species, and finally stored in the fridge, 4 °C.

*Dynamic Light Scattering (DLS)*: DLS measurements were performed on a Zetasizer Nano ZS (Malvern Instruments, UK) using disposable acryl cuvettes. The intensity of scattered light was recorded at a fixed angle of 173°, with a laser light wavelength of 633 nm employed for the scattering experiments. Standard data analysis procedures using the onboard software (Nanosoftware V3.30, Malvern Instruments, UK) were followed. The viscosity and refractive index values were extracted from the software and subsequently utilized to generate plots in Origin (OriginLab Corporation, USA).

*Optical Spectroscopy*: Steady-state emission spectra and time-resolved emission profiles were captured employing a JASCO FP-8300 fluorescence spectrometer, which equipped a 450 W xenon arc lamp, double-grating excitation, and emission monochromators. Emission spectra were corrected with source intensity (lamp and grating) and the emission spectral response (detector and grating) by standard correction curves.

Time-resolved measurements were conducted with a Horiba Jobin-Yvon IBH FL-322 Fluorolog 3 spectrometer using time-correlated single-photon counting (TCSPC) electronics FluoroHub. Pulsed laser diodes LDH-P-C-373 ($\lambda$ = 373 nm, pulse duration 1.2 ns, max repetition rate 1 MHz) and LDH-P-C-255 ($\lambda$ = 255 nm, pulse duration < 1.2 ns, max repetition rate 1 MHz) were employed for sample excitation, mounted directly on the sample chamber at 908. Photon collection was facilitated using a TBX picosecond photon detection module single-photon-counting detector. Data acquisition was performed using commercially available DataStation software (Horiba Jobin-Yvon), with subsequent analysis conducted using the DAS56 software (Horiba Jobin-Yvon). Quantum yield measurements were carried out using a Fluorolog-3 spectrofluorometer equipped with a Quanta-Φ integrating sphere accessory. Data acquisition was managed by FluorEssence software (Horiba Jobin-Yvon) version 3.5. All cuvettes were equipped with a stirrer allowing rapid mixing.

*Atomic Force Microscopy (AFM)*: The thickness of the polymer brush coatings was measured using a Dimension Icon (Bruker, Germany) AFM. A scratch on the polymer brush substrate by a metal tweezer was analyzed in tapping mode in air with aluminum reflex coating silicon tip (40 N m$^{-1}$, 300 kHz, Tap300AI-G, Budgetsensors, Germany). Each sample was measured at three different sites to check the consistency of the outcome.

*Immobilization of Vesicles*: For vesicle immobilization, 50 μL of 1% streptavidin in PBS was incubated onto the micropatterned polymer brush-coated substrates for 30 min to allow streptavidin to bind to the biotinylated parts of the polymer brush, followed by 7 times of pipetting on and off 100 μL PBS to wash away unbound streptavidin. Subsequently, the streptavidin-DBCO-Biotin patterns were incubated with 50 μL of the vesicle solution with encapsulated CB8·MDAP for 20 h. After incubation, the micro-pattern was washed with PBS 10 times via the method mentioned above to remove unbound vesicles. The incubated micropatterns (with PBS on them) were then imaged with an inverted fluorescence microscope.

*Incubation of Analytes*: The immobilized vesicle arrays were initially coated with 50 μL of the PBS buffer. Then the substrate was transferred onto a heating plate that reached the predetermined temperature. Subsequently, a specific amount (50–100 μL) of vesicle solution was injected into the droplet by introducing the pipette tip into the droplet. After the desired incubation time, the samples were washed by pipetting on and off PBS to remove the analyte. Then the sample was transferred (with PBS on) to an inverted fluorescence microscope for analysis.

*Fluorescence Microscopy*: The fluorescence imaging was performed on a Nikon Eclipse Ti2 inverted fluorescence microscope (Nikon, Japan) equipped with an Intensilight illumination, a Nikon DS Qi2 camera, and DIA, Cy3, GFP, and DAPI filter sets (Nikon Y-2E/C).

*Statistical Analysis*: All data presented in this study are reported as means or means ± standard deviation. Fluorescence intensity values were acquired using the onboard software (NIS Elements AR 5.02.00, Nikon) of the microscope. Specifically, five areas of the array or the background were selected using the area pickup function, and the mean intensity for each array or background was recorded. These intensities were subsequently utilized to calculate the mean intensity and relative intensity ($I/I_{background}$). The original data pertaining to contact angle (WCA), and thickness (by AFM) were obtained by measuring five random points on each sample. Means and standard deviations were computed using the STDEVA formula in Microsoft Excel and using Origin 2018b 64Bit to compile figures. The Gauss fitting function in Origin 2018b 64Bit was used to analyze the DLS data.

## Supporting Information

Supporting Information is available from the Wiley Online Library or from the author.

## Acknowledgements

This work was carried out with the support of the Karlsruhe Nano Micro Facility (KNMFi, www.knmf.kit.edu), a Helmholtz Research Infrastructure at Karlsruhe Institute of Technology (KIT, www.kit.edu). W.Y. acknowledges support from the China Scholarship Council fellowship (No. 202009110120, CSC, www.csc.edu.cn).

Open access funding enabled and organized by Projekt DEAL.

## Conflict of Interest

The authors declare no conflict of interest.

## Data Availability Statement

The data that support the findings of this study are available from the corresponding author upon reasonable request.

## Keywords

cucurbiturils, lipid vesicles, membrane permeability, microchannel cantilever spotting, polymer brushes

Received: March 3, 2024
Revised: April 12, 2024
Published online:

[1] C. Dias, *J. Nylandsted Cell Discov.* **2021**, *7*, 4.
[2] N. J. Yang, M. J. Hinner, in *Site-Specif. Protein Labeling* (Eds: A. Gautier, M. J. Hinner), Springer New York, New York, NY, **2015**, pp. 29.
[3] I. Hubatsch, E. G. E. Ragnarsson, P. Artursson, *Nat. Protoc.* **2007**, *2*, 2111.
[4] J. M. Reis, B. Sinko, C. H. R. Serra, *Mini-Rev. Med. Chem.* **2010**, *10*, 1071.
[5] H. Yu, Q. Wang, Y. Sun, M. Shen, H. Li, Y. Duan, *PLoS One* **2015**, *10*, 0116502.
[6] F. Biedermann, G. Ghale, A. Hennig, W. M. Nau, *Commun Biol* **2020**, *3*, 383.
[7] C. Zhong, C. Hu, R. Kumar, V. Trouillet, F. Biedermann, M. Hirtz, *ACS Appl. Nano Mater.* **2021**, *4*, 4676.
[8] C. G. Palivan, R. Goers, A. Najer, X. Zhang, A. Car, W. Meier, *Chem. Soc. Rev.* **2016**, *45*, 377.
[9] X. Zhang, M. Lomora, T. Einfalt, W. Meier, N. Klein, D. Schneider, C. G. Palivan, *Biomaterials* **2016**, *89*, 79.
[10] S. Rigo, G. Gunkel-Grabole, W. Meier, C. G. Palivan, *Langmuir* **2019**, *35*, 4557.
[11] D. Wu, S. Rigo, S. Di Leone, A. Belluati, E. C. Constable, C. E. Housecroft, C. G. Palivan, *Nanoscale* **2020**, *12*, 1551.
[12] Y. Ishizuka-Katsura, T. Wazawa, T. Ban, K. Morigaki, S. Aoyama, *J. Biosci. Bioeng.* **2008**, *105*, 527.
[13] S. M. Christensen, D. G. Stamou, *Sensors* **2010**, *10*, 11352.
[14] E. Boukobza, A. Sonnenfeld, G. Haran, *J. Phys. Chem. B* **2001**, *105*, 12165.
[15] G. Gunkel, M. Weinhart, T. Becherer, R. Haag, W. T. S. Huck, *Biomacromolecules* **2011**, *12*, 4169.
[16] J. Englert, L. Witzdam, D. Söder, M. Garay-Sarmiento, A. Joseph, A. M. Wagner, C. Rodriguez-Emmenegger, *Macromol. Chem. Phys.* **2023**, *224*, 2300306.
[17] J. Trmcic-Cvitas, E. Hasan, M. Ramstedt, X. Li, M. A. Cooper, C. Abell, W. T. S. Huck, J. E. Gautrot, *Biomacromolecules* **2009**, *10*, 2885.
[18] U. Bog, A. de los Santos Pereira, S. L. Mueller, S. Havenridge, V. Parrillo, M. Bruns, A. E. Holmes, C. Rodriguez-Emmenegger, H. Fuchs, M. Hirtz, *ACS Appl. Mater. Interfaces* **2017**, *9*, 12109.
[19] R. Kumar, B. Yang, J. Barton, M. Stejfova, A. Schäfer, M. König, P. Knittel, P. Cigler, M. Hirtz, *Adv. Mater. Interfaces* **2022**, 2201453.
[20] J. Striebel, M. Vorobii, R. Kumar, H.-Y. Liu, B. Yang, C. Weishaupt, C. Rodriguez-Emmenegger, H. Fuchs, M. Hirtz, K. Riehemann, *Adv Nanobiomed Res* **2021**, *1*, 2000029.
[21] B. Yang, Y. Wang, M. Vorobii, E. Sauter, M. Koenig, R. Kumar, C. Rodriguez-Emmenegger, M. Hirtz, *Adv. Mater. Interfaces* **2022**, *9*, 2102325.
[22] C. E. Neri-Cruz, F. M. E. Teixeira, J. E. Gautrot, *Chem. Commun.* **2023**, *59*, 7534.
[23] V. Sindelar, M. A. Cejas, F. M. Raymo, W. Chen, S. E. Parker, A. E. Kaifer, *Chemistry* **2005**, *11*, 7054.
[24] M. Nilam, S. Karmacharya, W. M. Nau, A. Hennig, *Angew. Chem., Int. Ed.* **2022**, *61*, e202207950.
[25] F. Biedermann, D. Hathazi, W. M. Nau, *Chem. Commun.* **2015**, *51*, 4977.
[26] Y. Liu, D. Liu, L. Zhu, Q. Gan, X. Le, *Food Res Int* **2015**, *74*, 97.
[27] R. L. Biltonen, D. Lichtenberg, *Chem. Phys. Lipids* **1993**, *64*, 129.
[28] A. S. Ulrich, M. Sami, A. Watts, *Biochim Biophys Acta* **1994**, *1191*, 225.
[29] L. Gross, M. Beals, S. Harrell, *QUBES Educ. Resour.* **2019**, https://doi.org/10.25334/Q4NF2G.
[30] A. C. Chakrabarti, D. W. Deamer, *Biochim Biophys Acta* **1992**, *1111*, 171.
[31] A. D. Bangham, M. M. Standish, J. C. Watkins, *J. Mol. Biol.* **1965**, *13*, 238.